COMMUNICATION

1D oriented attachment of calcite nanocrystals: formation of single-crystalline rods through collision

Mihiro Takasaki,[a] Yuki Kimura,[b] Tomoya Yamazaki,[b] Yuya Oaki[a] and Hiroaki Imai*[a]

The oriented attachment of calcite, which is a main component of biominerals, was experimentally demonstrated in an aqueous system at ambient temperatures. Calcite nanoblocks $\sim$50 nm in size were prepared by carbonation of $Ca(OH)_2$. One-dimensional (1D) alignment of the calcite nanoblocks was induced at ambient temperatures under a basic condition (pH $\sim$ 12), and single-crystalline rods over 1 μm were then formed through elongation in the *c* direction. The oriented attachment of the nanoscale building blocks was enhanced by increasing the collision frequency with stirring of the system, but was halted under a neutral pH condition with further carbonation. The controllable non-classical growth mode of calcium carbonate nanocrystals would provide significant information for biogenic and biomimetic mineralization in aqueous solutions.

In classical models, crystals are enlarged through ion-by-ion addition routes. According to the well-known Ostwald ripening mechanism, large particles grow by the addition of ions supplied at the expense of smaller particles in chemical solution systems. In contrast, the oriented attachment of nanocrystals is proposed as an alternative non-classical pathway for crystal growth.[1] Since Penn and Banfield presented a new crystal growth mechanism involving the attachment between two or more nanocrystals,[2] various experimental results have demonstrated crystal growth by the particle-by-particle addition route.[3–8] One-dimensional (1D) nanostructures were synthesized by the oriented attachment of nanocrystals of PbSe,[3] ZnO,[4] TiO_2,[5,6] and CeO_2.[7] Notably, the single-crystalline nanorods of PbSe and ZnO clearly formed through 1D alignment of their single particles. The formation process of the specific shapes through the oriented attachment was observed clearly in nanocrystal systems of metal oxides and chalcogenides in non-aqueous systems. Many reports have

discussed the non-classical routes for ionic crystals, such as carbonates and sulfates in aqueous solutions.[9–11] Nevertheless, oriented attachment was proposed on the basis of the presence of the single-crystalline configuration. Convincing studies with crucial evidence, such as capturing the decisive moment or aging variation, are required for clarification of the oriented attachment. However, direct observation of the oriented attachment is generally difficult with the coexistence of dissolution–deposition processes in nanometric systems. The solubility of several ionic crystals, such as $CaCO_3$, is not negligible in aqueous solutions. Therefore, the influence of dissolution–deposition processes on the final morphology are hardly excluded in nanometric systems. Consequently, SEM and TEM observation of the final morphology cannot be direct experimental evidence of the oriented attachment of ionic crystals. Moreover, the oriented attachment observed in the previous works cannot be controlled by the conditions. In the current study, we demonstrate the controllable oriented attachment of $CaCO_3$ nanocrystals in an aqueous system by changing the basicity and collision frequency at ambient temperatures. Here, we succeeded *in situ* TEM observation of the 1D oriented attachment using calcite nanocrystals prepared by carbonation of $Ca(OH)_2$. The direct evidence has been obtained in the present system because the rate of oriented attachment was relatively low and controlled by changing pH of the dispersion. Moreover, enhancement of the elongation of calcite by collision supports strongly the oriented attachment of nanocrystals.

In various $CaCO_3$-based biominerals, mesoscopic granular textures consisting of oriented nanocrystals have been observed with the incorporation of biological macromolecules.[12–16] The biogenic $CaCO_3$ crystals are composed of bridged nanograins that are arranged in the same crystallographic direction. The formation of bridged nanocrystals and mesocrystal structures similar to biominerals is usually ascribed to crystal growth by the control of organic molecules.[17–19] Biomimetic or bioinspired mineralization of $CaCO_3$ by artificial means is a well-known method to synthesize textured crystals, including mesocrystals.[19] Several routes to the textured crystals and mesocrystals

[a]*Department of Applied Chemistry, Faculty of Science and Technology, Keio University, 3-14-1 Hiyoshi, Kohoku-ku, Yokohama 223-8522, Japan. E-mail: hiroaki@applc.keio.ac.jp*

[b]*Institute of Low Temperature Science, Hokkaido University, Kita-19, Nishi-8, Kita-ku, Sapporo, Hokkaido 060-0819, Japan*

have been proposed to involve the oriented attachment of polymer-stabilized nanoparticles[20,21] and stepwise crystal growth with mineral bridges connecting nanoparticles.[22] Addadi and co-workers proposed that the textured $CaCO_3$ crystals are produced through a solid-state transformation of amorphous $CaCO_3$ (ACC) involving nanoparticle accretion.[23] In spite of these efforts, the formation mechanism of biogenic and biomimetic textured crystals and mesocrystals has not yet been fully revealed on the basis of experimental results.

In the present work, we monitored change in the morphology of calcite nanocrystals produced by carbonation of a $Ca(OH)_2$ dispersion under various conditions. Although the calcite nanocrystals were stably dispersed at a neutral pH region, we observed elongation of the crystals through the oriented attachment of the nanoblocks under a basic condition. The oriented attachment of the nanoscale building blocks was enhanced by increasing the collision frequency with stirring of the system. This is the first report on direct experimental evidence of the controllable 1D oriented attachment for the formation of $CaCO_3$ nanorods, which are regarded as building blocks of various biominerals.[14,15,24]

Calcite nanoblocks were synthesized in a 200 cm^3 aqueous dispersion of 42.5 g dm^{-3} $Ca(OH)_2$ through carbonation by the introduction of CO_2 at a rate of 3 dm^3 min^{-1}. The pH of the dispersion (~13) started to decrease when the carbonation reaction finished. The dispersion was then adjusted to pH 12 and 7 by the further introduction of CO_2 and was maintained at a constant temperature in the range of 4–90 °C. We monitored the pH value of the dispersion continuously with a pH meter (DKK-TOA GST-2739C, Japan) during the carbonation. We analyzed nanograins obtained by drying the filtered dispersion with X-ray diffraction (XRD, Rigaku MiniFlex II, Japan), scanning electron microscopy (SEM, Hitachi S-4700, Japan and JEOL JSM-7600F, Japan, operated at 1.0–5.0 kV), and transmission electron microscopy (TEM, FEI Tecnai F20, USA, operated at 200 kV) with selective area electron diffraction (SAED). The dispersion was dropped on a copper grid covered with a collodion film for TEM observation. We observed the morphological evolution of the nanograins in the dispersion. The oriented attachment of calcite nanoblocks was directly observed using *in situ* Fluid Reaction TEM (*in situ* FR-TEM, JEOL JEM-2100F, Japan, operated at 200 kV). For the observation, we used a "Poseidon" fluid reaction cell holder (Protochips, USA) with two input and one output ports. The fluid reaction cell consists of a pair of semiconductor-based plates with an amorphous silicon nitride window and 500 nm-thick spacer to form the flow path of the aqueous dispersion.

Calcite nanoblocks ~50 nm in size were found to be synthesized in a dispersion at pH 12 through the carbonation of $Ca(OH)_2$ according to SEM and TEM images and the XRD pattern (Fig. 1). Since the fast Fourier transform (FFT) spots corresponding to the lattice fringes of calcite were observed by high-resolution TEM (HRTEM), the single-crystalline grains were roughly covered with the {104} planes.

The dispersion of the calcite nanoblocks adjusted to pH 12 was maintained at a constant temperature in the range of 4–90
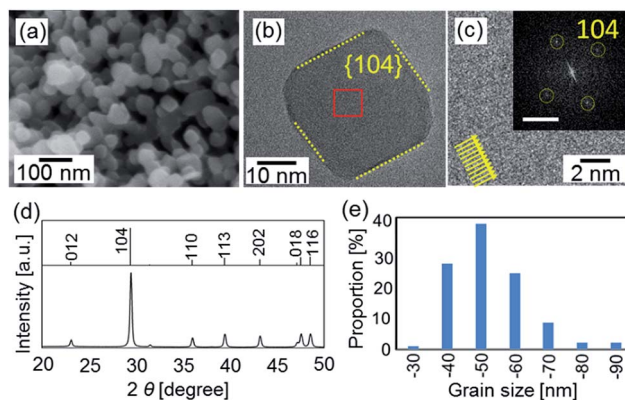

Fig. 1 SEM (a) and HRTEM (b and c) images, a typical XRD pattern (d), and grain-size distribution (e) of nanocrystals in a dispersion at pH 12 after carbonation. (c) An enlarged image of the red square area in (b) with its FFT pattern. The size distribution was estimated from SEM images.

°C. We found the gradual formation of nanorods from the calcite nanoblocks in the basic aqueous system below 60 °C (Fig. 2). The nanometric rods elongated up to ~500 nm in the dispersion stirred for 120 h (Fig. 2a), whereas the length increased slowly up to ~200 nm in 720 h without stirring (Fig. 2b). Therefore, stirring of the dispersion enhanced the elongation of the nanometric rods. This means that the collision frequency influenced the crystal growth. The maximum length of the rods obtained in the dispersion stirred for more than 336 h was over 2 μm (Fig. 3). On the other hand, the width of the rods was unchanged with the elongation. The calcite rods were confirmed to be a single crystal elongated in the *c* direction according to the presence of a continuous lattice in the HRTEM image and its FFT pattern (Fig. 2c).

The presence of the necks suggests that the single-crystalline rods were formed by 1D oriented attachment of the primary nanocrystals (TEM images in Fig. 2 and 3). We observed directly 1D oriented attachment of calcite nanoblocks in the basic dispersion using *in situ* FR-TEM. Fig. 4a shows three adjacent nanoblocks which were separated by tiny spaces in the dispersion after the carbonation. These nanoblocks were attached with each other after several minutes (Fig. 4b and c). This is experimental evidence of the occurrence of attachment of the nanoblocks in the liquid medium. Unfortunately, we could not evaluate crystallographic orientation of the adjacent nanoblocks because the crystal grains were easily damaged in the liquid medium under an intense irradiation of the electron beam.

We evaluated the crystallographic orientation from HRTEM images of the nanoblocks on a copper grid. Fig. 5a shows the attachment of adjacent nanocrystals as the first step of the elongation of the nanorods. These grains were crystallographically connected in the *c* direction through a bridge after collision. We also observed attached grains with a defined boundary of the *c* planes (Fig. 5b). This suggests that the attachment of the calcite nanocrystals mainly occurred through the *c* planes. Occasionally, there was a slight change in the *c* direction at
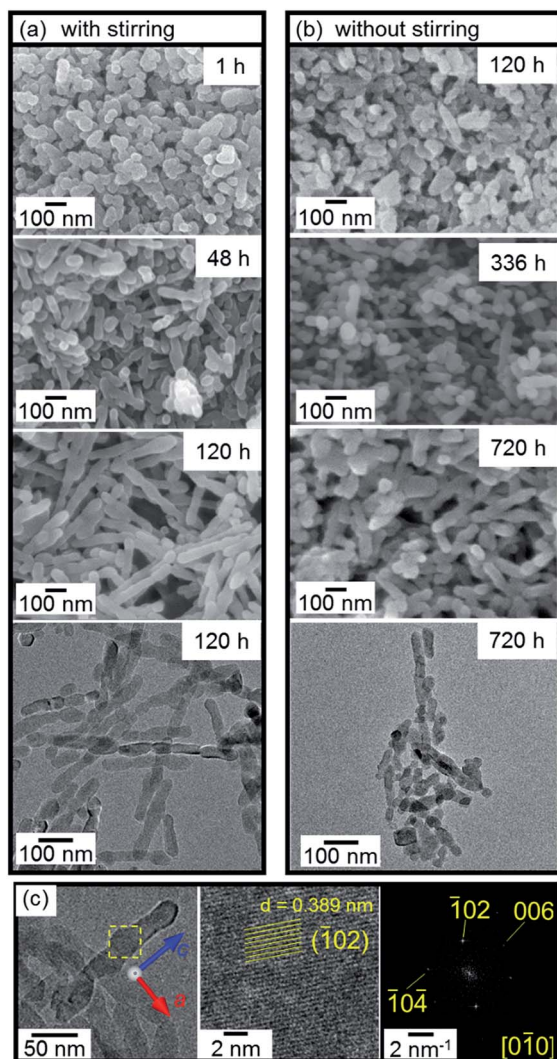
Fig. 2 SEM and TEM images of the variation of nanocrystals in aqueous dispersions at pH 12 and at 25 °C with (a) and without (b) stirring. (c)TEM and HRTEM images of elongated nanocrystals in a dispersion maintained at 25 °C for 720 h and the FFT pattern of the lattice in the HRTEM image.

a boundary between two calcite grains (Fig. 5c). The presence of the misorientation at the boundary can be explained by the particle-by-particle growth process but not by the ion-by-ion route.
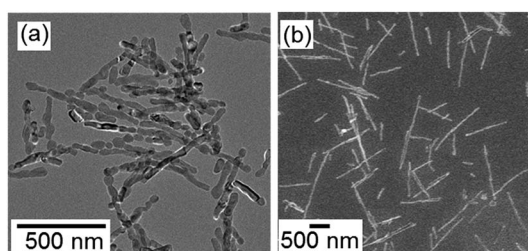

Fig. 3 TEM (a) and SEM (b) images of long rods obtained at 25 °C after stirring for 336 h (a) and 720 h (b).
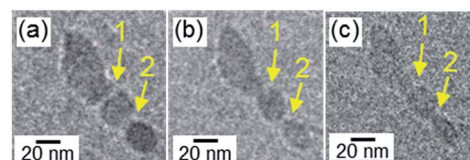

Fig. 4 *In situ* FR-TEM images for the oriented attachment of adjacent nanocrystals. Tiny spaces at boundary 1 and 2 observed in (a) disappeared after 15 min (b) and 35 min (c), respectively.

The nanocrystals were separated by centrifugation and were then redispersed in ethanol. After stirring at 4 °C, the formation of the nanorods was observed even in the non-aqueous medium (Fig. 6). Because the solubility of ionic crystals in ethanol is several orders of magnitude lower than that in water, the dissolution–deposition process is negligible in ethanol. Thus, the oriented attachment is inferred to be dominant for the formation of the 1D structure.

We decreased pH of the dispersion by the further introduction of CO_2. The nanocrystals were stably dispersed in an aqueous medium at pH 7 for more than 720 h below 25 °C. This means that the oriented attachment was halted by changing the basicity. The high dispersivity is ascribed to the surface charge of the nanocrystals because the pH value of the dispersion was far from the isoelectric point (pH 11.5).

Homogeneous expansion of the crystal grains occurred in the basic dispersions at 90 °C (Fig. 7). Rhombohedral facets of calcite covered with {104} planes were partially observed on the enlarged grains. The isotropic growth may be based on 3D oriented attachment of the nanoblocks. Further morphology changes in the calcite grains forming the facets would be ascribed to thermally enhanced surface diffusion or a dissolution–redeposition process localized near the surface.
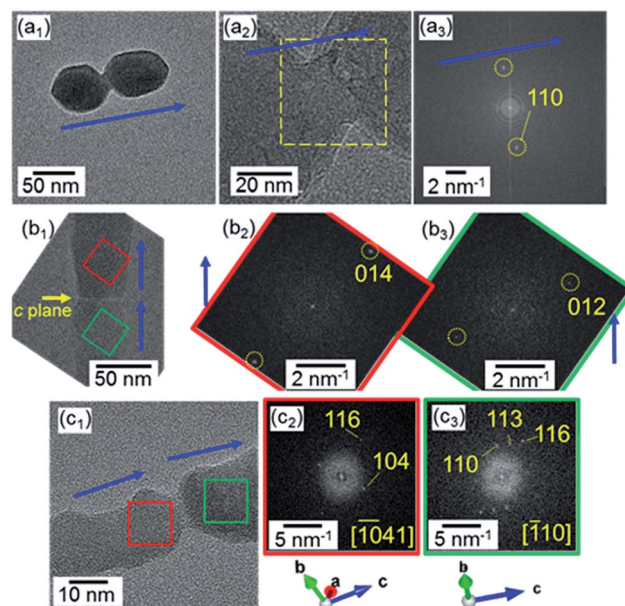

Fig. 5 HRTEM images ($a_{1,2}$, b_1, c_1) and their FFT patterns (a_3, $b_{2,3}$, $c_{2,3}$) for the attachment of two adjacent nanocrystals. Blue arrows indicate the c direction of calcite.
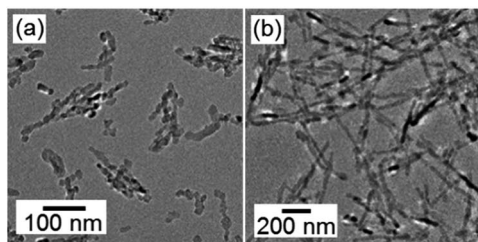
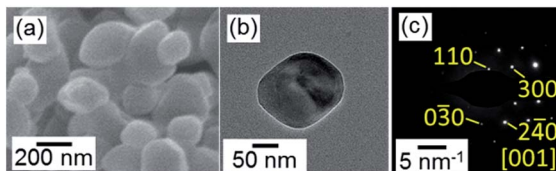**Fig. 6** TEM images of nanorods formed in ethanol after stirring at 4 °C for 120 h (a) and 720 h (b).

Fig. 7 SEM (a) and TEM (b) images and SAED (c) of calcite nanocrystals in a basic dispersion (pH 12) kept at 90 °C for 504 h.

Fig. 8 shows schematic illustrations of the formation mechanism for calcite nanorods through oriented attachment. Anionic and cationic planes in the calcite lattice are alternatively stacked in the *c* direction (Fig. 8a). The average surface charge of calcite crystals is negative in the entire pH region outside of the isoelectric point (pH 11.5) in the $CaCO_3$–H_2O–CO_2 system.[25] Under a neutral condition prepared by the additional introduction of CO_2, the attachment of calcite nanograins is inhibited by the repulsion of their surface charge (Fig. 8b). However, the *c* planes of the nanograins are deduced to be charged positively or negatively near the isoelectric point. The coulombic interaction promotes the attachment of the *c* faces of
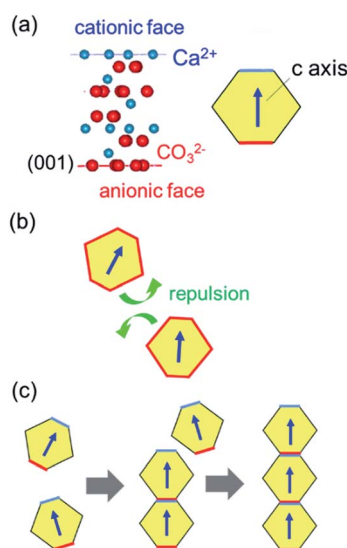
the calcite nanocrystals and then produces their 1D alignment (Fig. 8c). Stirring of the dispersion enhances the attachment because the collision frequency of the nanocrystals increases. On the other hand, the uncharged side faces suppress the oriented attachment perpendicular to the *c* axis. The 1D oriented attachment of calcite nanoblocks is induced under a basic condition and enhanced by increasing the collision frequency. Therefore, the controllable oriented attachment is achieved under ambient conditions.

Oriented attachment has been proposed as a formation route of mesostructures in $CaCO_3$-based biominerals as well as molecular controlled crystal growth. However, direct experimental evidence of the oriented attachment has hardly shown in previous works. In the current study, we clearly showed crystal growth of $CaCO_3$ by oriented attachment nanocrystals. Our findings on the controllable non-classical crystal growth of calcite, which is a main component of biominerals, would be helpful for understanding biogenic and biomimetic mineralization processes.

In summary, we monitored changes in the morphology of calcite nanocrystals in an aqueous system and found that the formation of single-crystalline nanorods elongated in the *c* direction under a basic condition at a constant temperature in the range of 4–60 °C. The elongation was clearly observed at relatively low temperatures whereas homogeneous expansion of the nanocrystals occurred at a high temperature above 75 °C. The specific crystal growth was observed not only in the aqueous medium but also in an ethanol dispersion. Therefore, the elongation of calcite is ascribed to the 1D oriented attachment of nanoscale building blocks. The attachment is advanced by increasing the collision frequency and inhibited under the neutral condition.

Acknowledgements

References

1 H. Cölfen and S. Mann, *Angew. Chem., Int. Ed.*, 2003, **42**, 2350.
2 R. L. Penn and J. F. Banfield, *Geochim. Cosmochim. Acta*, 1999, **63**, 1549.
3 W. Koh, A. C. Bartnik, F. W. Wise and C. B. Murray, *J. Am. Chem. Soc.*, 2010, **132**, 3909.
4 C. Pacholski, A. Kornowski and H. Weller, *Angew. Chem., Int. Ed.*, 2002, **41**, 1188.
5 H. Wang, Y. Liu, Z. Liu, H. Xu, Y. Deng and H. Shen, *CrystEngComm*, 2012, **14**, 2278.
6 Y. Zong, Y. Liu, W. Zhao, H. Zhang, B. Li, X. Zhou and H. Shen, *Electrochim. Acta*, 2015, **180**, 658.
7 N. Du, H. Zhang, B. Chen, X. Ma and D. Yang, *J. Phys. Chem. C*, 2007, **111**, 12677.

Fig. 8 Schematic illustrations of a calcite nanoblock with its ionic configuration (a), repulsion of nanoblocks under a neutral condition (b), and 1D oriented attachment of the nanoblocks in the *c* direction (c).

8 Y. Nakagawa, H. Kageyama, R. Matsumoto, Y. Oaki and H. Imai, *CrystEngComm*, 2015, **17**, 7477.

9 C. Rodriguez-Navarro, K. Kudłacz, Ö. Cizerc and E. Ruiz-Agudo, *CrystEngComm*, 2015, **17**, 58.

10 N. Gehrke, H. Cölfen, N. Pinna, M. Antonietti and N. Nassif, *Cryst. Growth Des.*, 2005, **5**, 1317.

11 L. Qi, H. Cölfen, M. Antonietti, M. Li, J. D. Hopwood, A. J. Ashley and S. Mann, *Chem.–Eur. J.*, 2001, **7**, 3526.

12 Y. Oaki, A. Kotachi, T. Miura and H. Imai, *Adv. Funct. Mater.*, 2006, **16**, 1633.

13 M. Kijima, Y. Oaki and H. Imai, *Chem.–Eur. J.*, 2011, **17**, 2828.

14 A. Hayashi, T. Watanabe and T. Nakamura, *Zoology*, 2010, **113**, 125.

15 M. Suzuki, T. Kogure, S. Weiner and L. Addadi, *Cryst. Growth Des.*, 2011, **11**, 4850.

16 S. Mann, *J. Chem. Soc., Dalton Trans.*, 1993, 1.

17 M. J. Olszta, S. Gajjeraman, M. Kaufman and L. B. Gower, *Chem. Mater.*, 2004, **16**, 2355.

18 Z. R. Tian, J. A. Voigt, J. Liu, B. Mckenzie, M. J. Mcdermott, M. A. Rodriguez, H. Konishi and H. Xu, *Nat. Mater.*, 2003, **2**, 821.

19 O. Grassmann and P. Löbmann, *Chem.–Eur. J.*, 2003, **9**, 1310.

20 F. Dang, K. Kato, H. Imai, S. Wada, H. Haneda and M. Kuwabara, *Cryst. Growth Des.*, 2011, **11**, 4129.

21 K. X. Yao, X. M. Yin, T. H. Wang and H. C. Zeng, *J. Am. Chem. Soc.*, 2010, **132**, 6131.

22 Y. Oaki, S. Hayashi and H. Imai, *Chem. Commun.*, 2007, 2841.

23 S. Raz, P. C. Hamilton, F. H. Wilt, S. Weiner and L. Addadi, *Adv. Funct. Mater.*, 2003, **13**, 480.

24 E. N. K. Clarkson, *Palaeontology*, 1973, **16**, 425.

25 P. Moulin and H. Roques, *J. Colloid Interface Sci.*, 2003, **261**, 115.